Extending the Patched-Conic Approximation to the Restricted Four-Body Problem

Thomas R. Reppert

Department of Aerospace and Ocean Engineering

Virginia Polytechnic Institute and State University

Blacksburg, VA 24061

Abstract

This paper presents an investigation of how to refine patched-conic orbit approximations with a restricted four-body orbit setup. By approximating an overall orbit as a series of two-body orbits, patched-conic approximations offer a greatly simplified way of analyzing missions. However, they are limited in their ability to fully represent a particular orbit. Therefore, we must use a numerical integration technique to more precisely describe interplanetary missions. By extending the patched-conic approximation to a restricted four-body problem, we achieve a more precise orbit transfer description. Taking into consideration the gravitational influences of the sun, Earth, and Mars at all times, we compute a spacecraft's transfer orbit from Earth to Mars. The integrator provides a more precise estimate of the state of the vehicle upon its arrival at Mars. The initial orbit conditions are adjusted and the effects upon the arrival state are measured. Also, the values of required departure burn are compared for the Hohmann solution, the patched-conic approximation, and the restricted four-body problem.

1 Introduction

A Hohmann transfer is an interplanetary mission that requires a change in true anomaly of 180 degrees. It is a particular type of minimum energy transfer orbit. In fact, the Hohmann transfer requires a minimum initial burn in order to reach the foreign planet.[2] The Hohmann is commonly used to transfer from one circular orbit to another. Thus, it is an attractive option for designing future missions from Earth to Mars.

Analytic solutions relating the planets' mean heliocentric orbit radii to the required departure burn have already been established.[4] These equations were developed chiefly through the application of conservation laws, including the conservations of both angular momentum and energy. But these solutions only provide a rough estimate of how to reach

Mars' sphere of influence. We desire a higher fidelity method for estimating the required initial burn. In addition, we seek a method which allows us to alter the departure orbit geometry and to analyze the effects upon the arrival at Mars.

The patched-conic approximation has thus been developed as a more accurate solution to interplanetary transfer description. It involves partitioning the overall transfer into several two-body problems. In other words, only one celestial body's influence is considered to be acting upon the spacecraft at all times. This approximation provides a much better understanding of the relation between the departure orbit and the overall transfer than the analytic Hohmann solution. However, the patched-conic approximation is still limited in that it only considers the gravity of one celestial body at a time.

When looking to design a real-time interplanetary mission from Earth to Mars, we seek a higher fidelity orbit description than the patched-conic approximation. The restricted four-body problem offers a more precise representation of the transfer orbit. Applied to a Hohmann transfer from Earth to Mars, the restricted four-body problem considers the gravitational influences of Earth, the sun, and Mars at all times. This orbit integration scheme presents a method of analyzing a highly non-linear transfer orbit without breaking the orbit into separate parts.

2   Patched-Conic Approximation

The patched-conic approximation offers an efficient method for describing interplanetary orbits. By partitioning the overall orbit into a series of two-body orbits, it greatly simplifies mission analysis. For each of the portions of an orbit, one gravitational force is assumed to be acting upon the spacecraft at a time.[2] To illustrate the efficiency of the patched-conic approximation, we partition the standard Hohmann transfer of a spacecraft traveling from Earth to Mars into three separate conic stages. During the initial portion of the voyage, we approximate the transfer as a hyperbolic departure orbit with its primary focus positioned at the center of the Earth. After escaping the Earth's sphere of influence, the spacecraft then enters its elliptic orbit about the sun. Following this second stage, the spacecraft enters Mars' sphere of influence. Once again, we approximate the motion as a hyperbolic orbit, this time with its focus located at the center of Mars.

2.1   Determining the Heliocentric Departure Velocity

A typical application of the patched-conic solution is to determine the approximate magnitude of Δv needed to complete a certain transfer mission. We first seek the necessary heliocentric velocity v_1 as the spacecraft leaves the Earth's sphere of influence. This particular velocity is illustrated in Figure 1. The v_1 necessary to complete the Hohmann
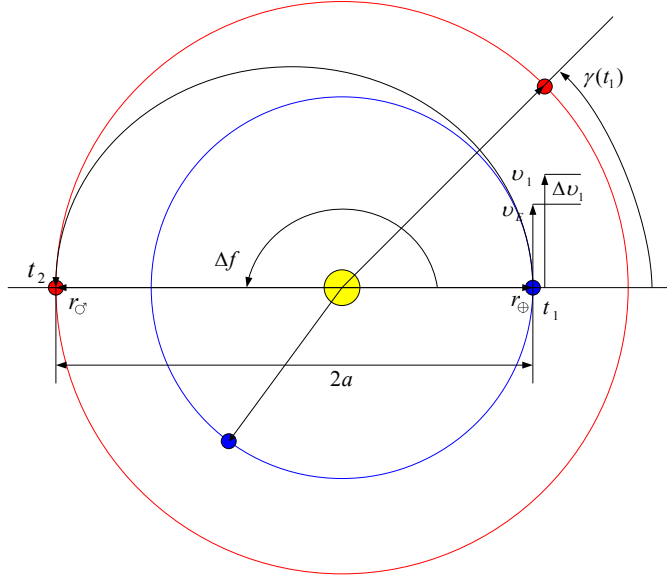
Figure 1.— Illustration of the Hohmann transfer from Earth to Mars.

transfer may be computed as

$$v_1 = \sqrt{\frac{2\mu_\odot}{r_\oplus + r_\mathars} \left(\frac{r_\mars}{r_\oplus}\right)}$$

(1)

where $\mu_\odot$ denotes the sun's gravitational coefficient, $r_\oplus$ denotes the Earth's mean orbit radius, and $r_\mars$ denotes Mars' mean orbit radius. For a complete derivation of Equation 1, consult Schaub and Junkins.[4] Once the heliocentric departure velocity is calculated, Δv_1 may be computed as

$$\Delta v_1 = v_1 - v_\oplus = v_\oplus \left(\sqrt{\frac{2r_\mars}{r_\oplus + r_\mars}} - 1\right)$$

(2)

where $v_\oplus$ is the Earth's mean heliocentric velocity, as shown in Figure 1. Because $r_\mars > r_\oplus$, the resulting Δv_1 will be positive.

2.2 Leaving Earth's Sphere of Influence

The following discussion offers a closer examination of how the spacecraft escapes Earth's sphere of influence. Figure 2 offers an illustration of the departure.

Throughout the following analysis, heliocentric velocities are expressed as v_i, while planet-centric velocities are denoted as ν_i. Because the spacecraft is required to converge to some velocity v_1 as it leaves Earth's sphere of influence, the departure orbit must be hyperbolic. The necessary Earth-relative velocity ν_1 at the limit of the sphere of influence
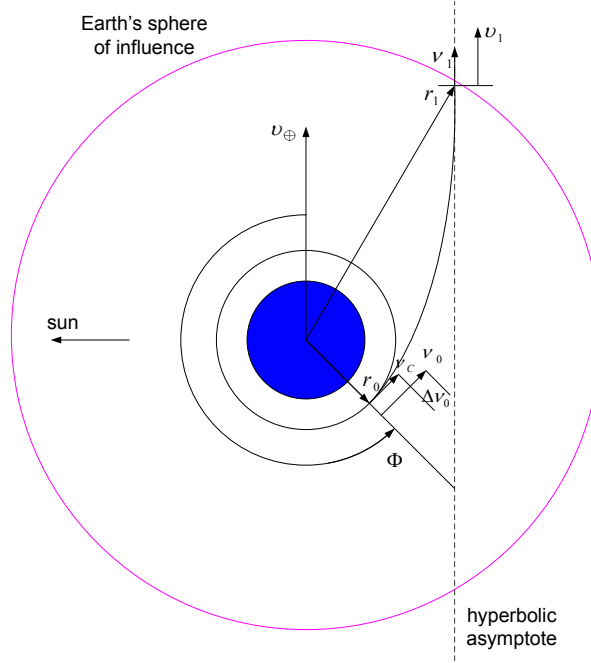
Figure 2.— Illustration of the hyperbolic departure from Earth's sphere of influence.

is computed as

$$\nu_1 = \upsilon_1 - \upsilon_\oplus \tag{3}$$

We can also use the vis-viva equation[4] to determine the Earth-relative velocity ν_1 as

$$\nu_1 = \sqrt{\frac{2\mu_\oplus}{r_1} - \frac{\mu_\oplus}{a_h}} \approx \sqrt{-\frac{\mu_\oplus}{a_h}} \tag{4}$$

where $\mu_\oplus$ denotes the Earth's gravitational coefficient and a_h corresponds to the semi-major axis of the departure hyperbola. We approximate $r_1 \approx \infty$ due to the assumption that the spacecraft trajectory asymptotically approaches its limiting value at time t_1. Therefore, we can relate the departure hyperbola's semi-major axis to either ν_1 or υ_1 via

$$a_h = \frac{-\mu_\oplus}{\nu_1^2} = -\frac{\mu_\oplus}{(\upsilon_1 - \upsilon_\oplus)^2} \tag{5}$$

Using the vis-viva equation once again, the Earth-relative speed ν_0 that the vehicle must have in order to initiate the hyperbolic transfer orbit at t_0 becomes

$$\nu_0 = \sqrt{\frac{2\mu_\oplus}{r_0} - \frac{\mu_\oplus}{a_h}} \tag{6}$$

where r_0 denotes the spacecraft's initial parking orbit radius about the Earth. After substituting the relation for a_h given in Equation 5, the speed ν_0 is expressed as

$$\nu_0^2 = \nu_1^2 + \frac{2\mu_\oplus}{r_0} \tag{7}$$

136

At this point, it is important to note that once ν_1 and r_0 are chosen for a particular mission, the corresponding patched-conic approximation for ν_0 is set.

In order to maintain its initial parking orbit about Earth, the spacecraft has a critical speed of

$$\nu_c = \sqrt{\frac{\mu_\oplus}{r_0}} \tag{8}$$

The initial burn required to begin the hyperbolic transfer is given as

$$\Delta\nu_0 = \nu_0 - \nu_c = \sqrt{2\nu_c^2 + \nu_1^2} - \nu_c \tag{9}$$

As shown in Figure 2, the point where the initial $\Delta\nu_0$ burn must be applied is defined via the angle Φ. For any transfer to an outer planet, the spacecraft's velocity should asymptotically align itself with Earth's heliocentric velocity. Thus, the burn angle Φ may be determined from the geometry of the departure hyperbola as

$$\Phi = \cos^{-1}\left(\frac{1}{e_h}\right) + \pi \tag{10}$$

where e_h refers to the eccentricity of the hyperbolic departure orbit. For a complete derivation of Equation 10, refer to Bate, Mueller, and White.[1] In order to find the departure eccentricity, the orbit's angular momentum must be analyzed.

2.3 Entering Mars' Sphere of Influence

We now analyze the patched-conic approximation of how the spacecraft enters Mars' sphere of influence. Figure 3 offers an illustration of the arrival orbit. It is typical for any spacecraft traveling to an outer planet to enter that planet's sphere of influence ahead of the planet. The spacecraft reaches the outer planet at the apoapses of the transfer orbit. Therefore, the spacecraft's speed will be less than that of the planet, allowing the planet to overtake it. Once again, using the vis-viva equation,[4] we find the heliocentric arrival velocity v_2 of the spacecraft to be

$$v_2 = \sqrt{2\mu_\odot\left(\frac{1}{r_\mars} - \frac{1}{r_\oplus}\right) + v_1^2} \tag{11}$$

When the spacecraft arrives at Mars, it will most likely cross Mars' sphere of influence with some heading angle σ_2.[1]. For a perfect Hohmann transfer, the value of σ_2 would be exactly equal to 0 degrees. To compute the spacecraft's Mars-centric velocity vector $\boldsymbol{\nu}_2$, Mars' heliocentric velocity must be subracted from that of the spacecraft:

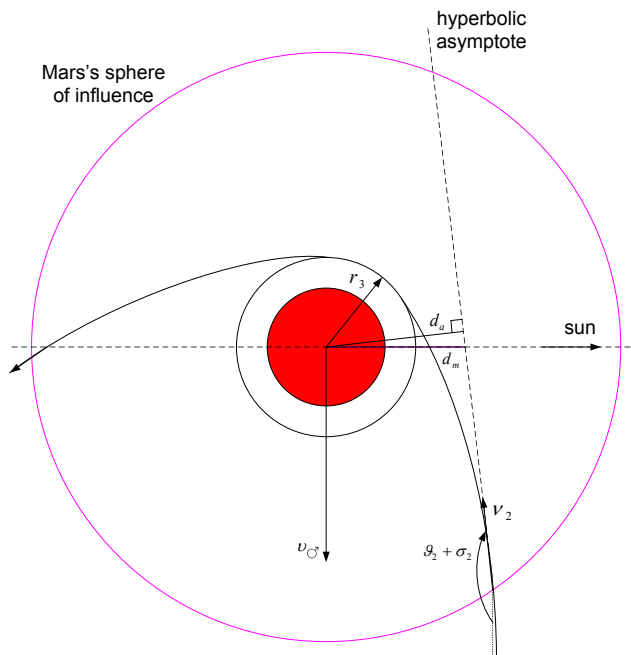$$\boldsymbol{\nu}_2 = \boldsymbol{v}_2 - \boldsymbol{v}_\mars \tag{12}$$

137

Figure 3.— Illustration of the hyperbolic arrival at Mars' sphere of influence.

Via the law of cosines, the magnitude of $\boldsymbol{\nu}_2$ is calculated as

$$\nu_2 = \sqrt{v_2^2 + v_{\circlearrowleft}^2 - 2v_2 v_{\circlearrowleft} \cos \sigma_2} \tag{13}$$

Identical to the process used to describe the departure orbit, we use the energy (vis-viva) equation to determine the semi-major axis of the arrival orbit through

$$\frac{1}{a_h} = \frac{2}{r_2} - \frac{\nu_2^2}{\mu_{\circlearrowleft}} \tag{14}$$

Making the patched-conic assumption that the spacecraft's approach orbit is hyperbolic, we approximate a_h as

$$a_h = -\frac{\mu_{\circlearrowleft}}{\nu_2^2} \tag{15}$$

where $r_2 \approx \infty$. If the Hohmann orbit were perfect, the spacecraft would impact the Martian surface. To avoid this occurence, the hyperbolic arrival trajectory is aimed such that it will miss Mars by some miss distance d_m, as shown in Figure 3. However, from the spacecraft's perspective, it is easiest to estimate the shortest distance d_a between the approach asymptote and Mars. Similar to the departure orbit, we examine the spacecraft's constant angular momentum in order to determine the arrival eccentricity e_h. The transfer mission is usually designed in such a way that the periapses radius is equivalent to the final parking orbit radius. Thus, the final orbit radius about Mars is uniquely determined once both the eccentricity e_h and arrival speed ν_2 are given. Because e_h depends upon the miss distance, the arrival is actually set with prescribed values of d_m and ν_2.

3   Restricted Four-Body Problem

In this section, we extend the patched-conic approximation to the restricted four-body problem. Taking into consideration the gravitational influences of the sun, Earth, and Mars at all times, we determine the spacecraft's transfer orbit from Earth to Mars. All orbital motion during the transfer is assumed to be planar. Also, the orbits of Earth and Mars are assumed to be circular.

3.1   Derivation of the Equations of Motion

Before beginning the numerical integration process, we must first derive the equations of motion that we wish to integrate. Figure 4 offers an illustration of the coordinate frames used to designate the state of the spacecraft for all time t. The $\mathcal{S}$: $\{\hat{\boldsymbol{s}}_1, \hat{\boldsymbol{s}}_2, \hat{\boldsymbol{s}}_3\}$ frame is an
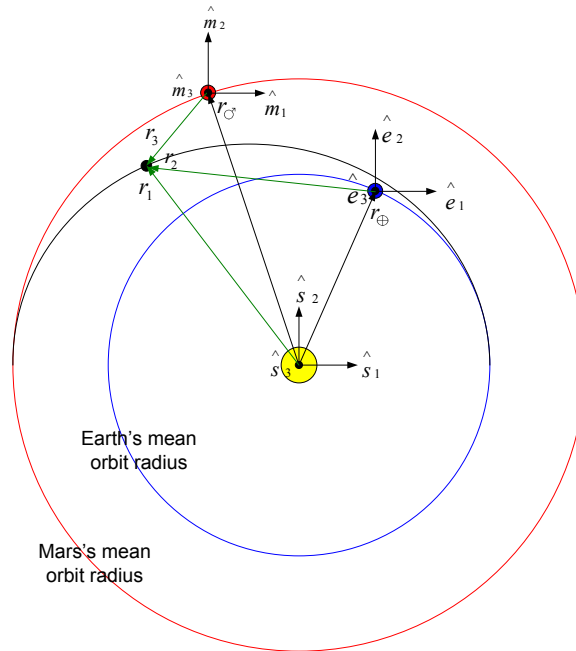

Figure 4.— Definition of the coordinate frames and position vectors used during the derivation of the spacecraft's equations of motion.

inertial frame centered at the sun. We make the assumption that the sun is stationary during the spacecraft's transfer orbit. The $\mathcal{E}$: $\{\hat{\boldsymbol{e}}_1, \hat{\boldsymbol{e}}_2, \hat{\boldsymbol{e}}_3\}$ frame is a non-rotating frame centered at Earth. This frame describes the state of the spacecraft with respect to Earth. In addition, the $\mathcal{M}$: $\{\hat{\boldsymbol{m}}_1, \hat{\boldsymbol{m}}_2, \hat{\boldsymbol{m}}_3\}$ frame is a non-rotating frame centered at Mars. In a similar manner, the M frame tracks the state of the spacecraft relative to Mars. As shown in Figure 4, the spacecraft's positions with respect to the sun, Earth, and Mars are labelled $\boldsymbol{r_1}$, $\boldsymbol{r_2}$, and $\boldsymbol{r_3}$, respectively.

For a general n-body problem, the total force $\boldsymbol{f}_i$ acting upon mass m_i, due to the other

$n - 1$ masses, is

$$\boldsymbol{f}_i = G \sum_{j=1}^{n} \frac{m_i m_j}{r_{ij}^3} (\boldsymbol{r}_j - \boldsymbol{r}_i) \tag{16}$$

where G is the universal gravitation constant. The term for which $i = j$ is to be omitted. Newton's Second Law of Motion states

$$\boldsymbol{f}_i = m_i \frac{d^2 \boldsymbol{r}_i}{dt^2} \tag{17}$$

Therefore, the n vector differential equations

$$\frac{d^2 \boldsymbol{r}_i}{dt^2} = G \sum_{j=1}^{n} \frac{m_j}{r_{ij}^3} (\boldsymbol{r}_j - \boldsymbol{r}_i) \tag{18}$$

along with appropriate initial conditions completely describe the motion of the system of n particles. Consult Battin for the complete derivation of Equation 18.[2] With the restricted four-body assumption, we neglect the gravitational effects of the spacecraft upon the three celestial bodies. We also treat the two planetary orbits as perfect circles. Thus, Equation 18 becomes

$$\ddot{\boldsymbol{r}}_1 + \frac{\mu_{\odot}}{r_1^3} \boldsymbol{r}_1 + \frac{\mu_{\oplus}}{r_2^3} \boldsymbol{r}_2 + \frac{\mu_{\mathrm{C}}}{r_3^3} \boldsymbol{r}_3 = 0 \tag{19}$$

where $\ddot{\boldsymbol{r}}_1$ represents the second inertial derivative of $\boldsymbol{r}_1$ with respect to time. Also, we have used the relation

$$\mu = G(m_1 + m_2) \tag{20}$$

in order to express the equations of motion of the spacecraft in terms of the three gravitational coefficients μ_i of the celestial bodies.

3.2 Numerical Integrator

A numerical integration technique is required in order to estimate the spacecraft's state vector over time. The integration technique chosen to perform this task is the Classical Fourth-Order Runge-Kutta Method.[3] Figure 5 offers an illustration of one iteration of the Fourth-Order Runge-Kutta Method. Using this method, we integrate the state variable as

$$\boldsymbol{y}_{i+1} = \boldsymbol{y}_i + \frac{1}{6}(\boldsymbol{k}_1 + 2\boldsymbol{k}_2 + 2\boldsymbol{k}_3 + \boldsymbol{k}_4)g \tag{21}$$

Because each of the $\boldsymbol{k}$'s represents a slope estimate, Equation 21 uses a weighted slope average to more efficiently determine the state vector at the future time t_{i+1}.[3]

At this point, it must be noted that we can use a variable time step in order to improve the efficiency of the Runge-Kutta integrator. As the spacecraft travels through either
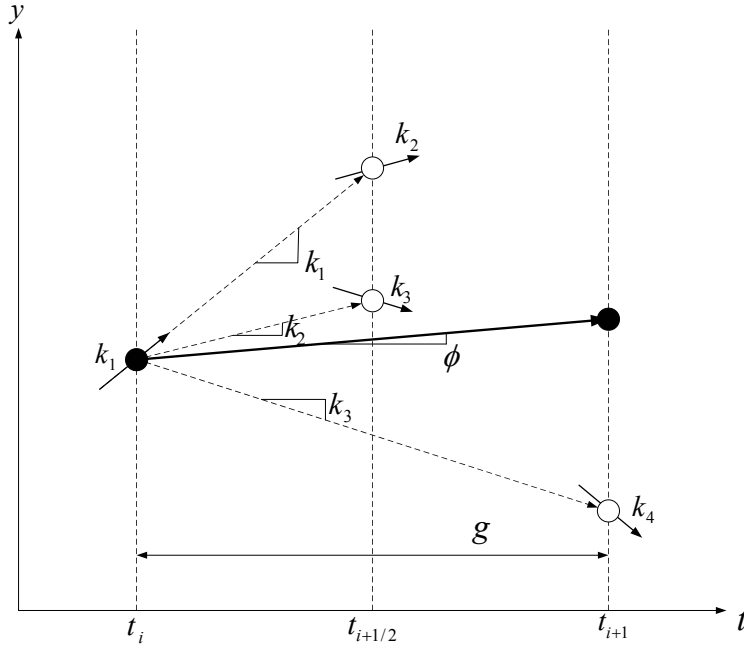
Figure 5.— Illustration of the calculation of slope estimates during one iteration of the Fourth-Order Runge-Kutta Method.

Earth's or Mars' sphere of influence, it accelerates at a much greater rate than during the heliocentric portion of the mission. Therefore, it is very computationally efficient to increase the integration time step g during the heliocentric portion of the transfer orbit.

4   Integration Results

We now examine the application of the four-body problem to the Hohmann transfer from Earth to Mars. The effect of varying certain initial conditions upon the development of the orbit is analyzed. Also, the values of necessary departure burn are compared for the Hohmann solution, the patched-conic approximation, and the restricted four-body problem.

4.1   Changing the Mars Offset Angle

There must exist some initial offset angle $\gamma(t_1)$ between Earth and Mars. If there were no initial offset angle, the spacecraft would perform the Hohmann transfer without ever entering Mars' sphere of influence. By altering the initial offset angle, we can examine the effect that it has upon the hyperbolic arrival orbit. Thus, we perform a series of restricted four-body integrations, varying this offset angle $\gamma(t_1)$. Figure 6 displays a group of arrival orbits for five different Mars offset angles. The planet-centric step size used to integrate the five different cases is 50 seconds. Increasing the initial offset angle noticeably varies the miss distance d_m between the spacecraft's projected trajectory and the sun direction. As $\gamma(t_1)$ is increased from 44.718 to 44.843 degrees, the miss distance
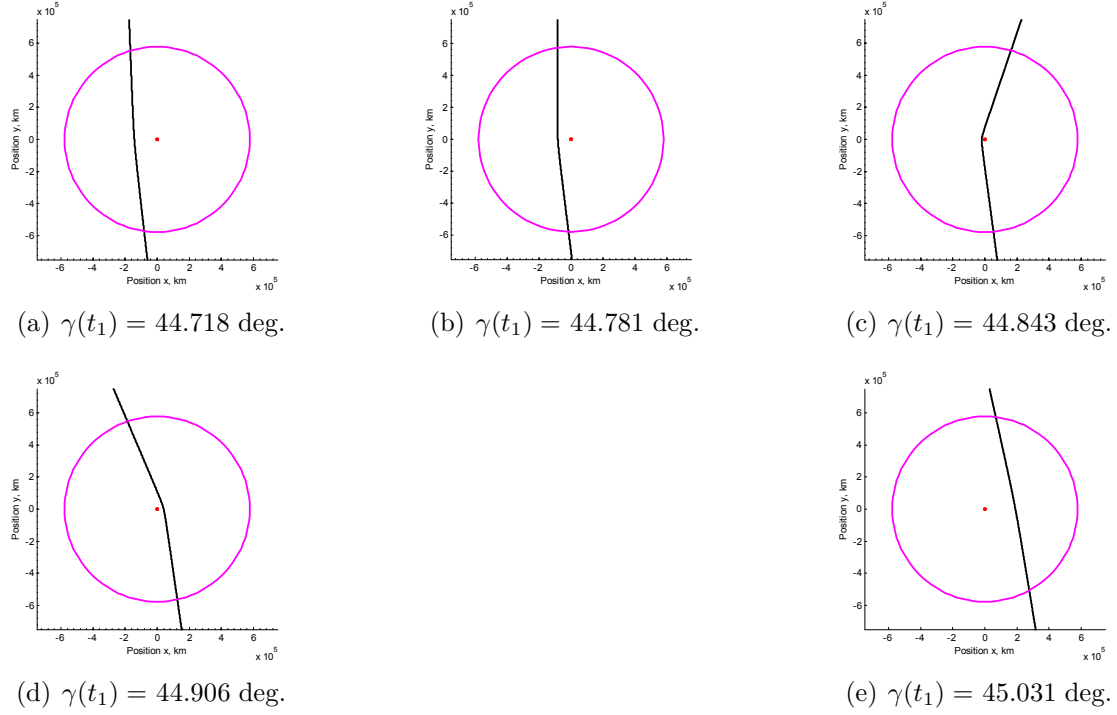
141

(a) $\gamma(t_1) = 44.718$ deg.   (b) $\gamma(t_1) = 44.781$ deg.   (c) $\gamma(t_1) = 44.843$ deg.

(d) $\gamma(t_1) = 44.906$ deg.   (e) $\gamma(t_1) = 45.031$ deg.

Figure 6.— Series of hyperbolic arrival orbits corresponding to five different initial offset angles between Earth and Mars. The x and y positions are taken relative to the Mars-centered frame $\mathcal{M}$. The step size g_h used is 50 seconds.

decreases and the eccentricity of the hyperbolic arrival increases. Once $\gamma(t_1)$ surpasses 44.843 degrees, the spacecraft begins performing counter-clockwise orbits about Mars. This effect is particularly important if we want to ultimately achieve a geostationary orbit about Mars.

Secondly, the changes in initial offset angle $\gamma(t_1)$ have a slight effect upon the arrival heading angle $\sigma_2 + \vartheta_2$. Note that, as the offset angle is increased from 44.718 to 45.031 degrees, the heading angle decreases from its initial value of roughly 180 degrees. The reason for this slight decrease in heading angle is that the spacecraft is now penetrating Mars' sphere of influence at an earlier time on its Hohmann transfer. Thus, the heading angle begins to regress from the ideal value of 180 degrees for a perfect Hohmann transfer.

4.2   Changing Mars' Heliocentric Orbit Radius

When we use the patched-conic approximation to estimate the necessary initial conditions for the Hohmann transfer, the arrival orbit overshoots Mars by roughly 4e+005 kilometers. Therefore, if we want to achieve a certain hyperbolic periapses radius r_3 about Mars, we must alter at least one initial condition. Referring to the patched-conic arrival orbit solutions presented in Section 2, we find that the r_3 parking radius depends upon the miss distance d_m and the velocity $\boldsymbol{\nu}_2$. The planar Hohmann transfer from Earth to Mars will always yield an arrival speed ν_2 roughly equal to 2.648 km/s, as calculated in

Section 2. Thus, to achieve a specific parking orbit radius about Mars, we alter the miss distance d_a until the necessary arrival geometry is obtained. One way to alter the miss distance d_a of the arrival hyperbola is to make small changes in Mars' heliocentric orbit radius. Using such a method, we determine what Martian heliocentric orbit radius will yield the miss distance d_a corresponding to the desired parking radius r_3. Figure 7 offers a flow chart illustrating the $r_{\mars}$ correction process.
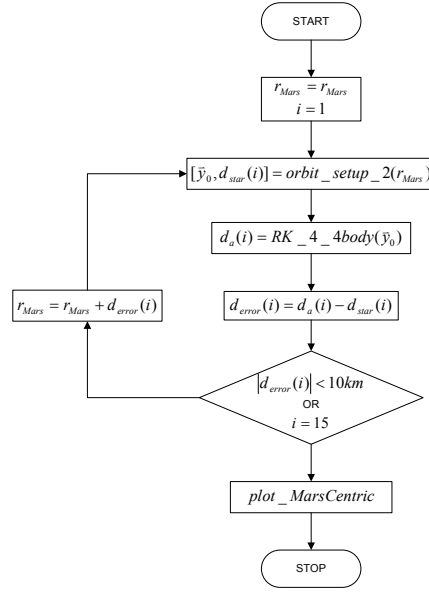

Figure 7.— Flow chart depicting the loop used to iteratively correct Mars' orbit radius $r_{\mars}$ in order to achieve the desired arrival parking radius r_3 about Mars.

The advantage of using a variable time step is accentuated when we perform the given iteration to achieve a unique arrival geometry. Figure 8 offers an illustration of both the uncorrected and corrected arrival orbit geometries. For the iterations performed, we set the desired Mars parking radius r_3 to 4000 km. The initial iteration yields a miss distance of roughly 4e+005 kilometers. But after seven iterations are performed, the miss distance is almost exactly equal to the necessary value d_{star} of 8142 kilometers. Both graphs of Figure 8 show the projection of the $\boldsymbol{\nu}_2$ velocity upon entry into Mars' sphere of influence as a blue line. This projection is used to calculate the perpendicular distance to the center of Mars, corresponding to the actual miss distance d_a. By the seventh iteration, the magnitude of d_{error} drops below 1 kilometer. Figure 8 illustrates how the seventh iteration yields an arrival orbit with a periapses radius r_3 of roughly 4000 kilometers. Thus, we have taken the restricted four-body problem and found a set of initial conditions that result in a desired final parking orbit radius about Mars.
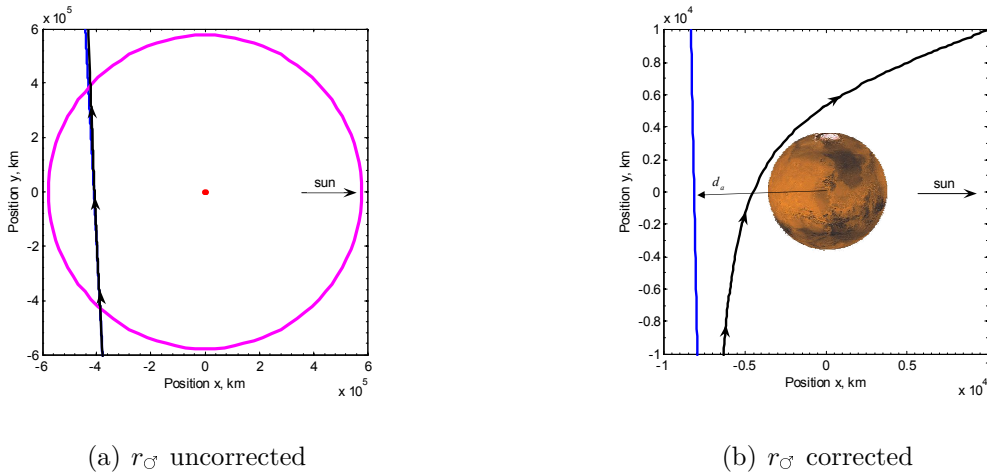
(a) $r_\mars$ uncorrected   (b) $r_\mars$ corrected

Figure 8.— Illustration of both the uncorrected and corrected arrival orbit geometries for the Mars orbit radius iteration. Values x and y are defined relative to the non-rotating Mars frame $\mathcal{M}$. Seven iterations were performed before achieving the final corrected arrival.

4.3 Comparison of Predicted Δv Values

So far, we have analyzed three different ways to estimate the necessary Δv value to travel from Earth to Mars on a Hohmann transfer. We first view the transfer orbit as a single elliptic orbit with a change in true anomaly of 180 degrees. Such an approximation treats the sun as the only gravitational influence upon the spacecraft during the transfer.

The second representation of the Hohmann transfer is as a series of two-body orbits about Earth, the sun, and Mars, respectively. Because we represent each portion of the orbit as a conic solution, we term this solution the patched-conic approximation. The patched-conic approximation allows us to take into account the gravity of Earth and Mars as the spacecraft travels through the planets' spheres of influence. However, this approximation ignores the gravitational effects of the planets when the spacecraft is traveling outside of their spheres of influence.

The final representation of the transfer orbit is as a restricted four-body orbit. Thus, we take the gravity of Earth, the sun, and Mars into consideration for the duration of the entire transfer orbit. We also examine the effects of altering certain departure orbit conditions upon the arrival orbit. More specifically, we determine the required Δv to achieve a particular periapses radius r_3 about Mars. Such a calculation cannot be made when examining the orbit using either the Hohmann approximation or the patched-conic approximation. Table 1 provides a listing of the Δv estimates corresponding to each of the three Hohmann transfer representations.

Note that the difference in required Δv values lies mostly in going from the general Hohmann approximation to the patched-conic approximation. However, integrating the restricted four-body problem allows us to determine the minute change in Δv that

144

Orbit Approximation	Δv (km/s)
Hohmann Transfer	2.943
Patched-Conic	3.432
Restricted Four-Body	3.428

Table 1.— Table showing the differences in required Δv estimates for the Hohmann transfer, patched-conic approximation, and restricted four-body problem. The value of Δv for the four-body approximation corresponds to a desired Mars parking orbit radius r_3 of 4000 km.

yields the desired Mars periapses radius of 4000 km. Such minute details are extremely important when attempting to establish a true interplanetary mission plan.

5   Conclusion

The original analytic solution to the Hohmann transfer from Earth to Mars offers a crude estimate of the Δv required to perform the transfer. Because it neglects the gravitational effects of both Earth and Mars, this orbit solution cannot achieve the same accuracy as the patched-conic approximation.

The patched-conic approximation provides a much better estimate of the Δv required to reach Mars on a Hohmann transfer. Its consideration of the planets' gravitational influences as the spacecraft travels through their spheres of influence makes this solution much more credible than the simple Hohmann solution. By breaking the entire orbit into three separate conic solutions, this approximation shows the effects of the departure orbit geometry on both the elliptic transfer and hyperbolic arrival.

The restricted four-body integration scheme allows us to view the Hohmann transfer from Earth to Mars as one propagated orbit. Thus, while taking into consideration the gravity of Earth, the sun, and Mars for all time, we can analyze the effects of altering certain initial conditions upon the arrival orbit. In addition, we can determine the necessary departure burn to achieve a desired parking orbit radius r_3 about Mars. The patched-conic approximation does not allow for such precise orbit modeling.

One idea for future work is to examine the applicability of the established four-body integrator to other interplanetary missions. The sensitivity of the four-body integrator to perturbations of these different orbits could then be analyzed. Still other future work could focus on increasing the accuracy of the presented four-body orbit modeling scheme. For instance, atmospheric drag is a disturbance that must be considered for both the departure and arrival orbits. Much work remains in developing an orbit modeling scheme that presents what would actually occur in a real-time transfer from Earth to Mars.

References

[1] Roger R. Bate, Donald D. Mueller, and Jerry E. White. *Fundamentals of Astrodynamics.* Dover Publications, Inc., New York, NY, 2005.

[2] Richard H. Battin. *An Introduction to the Mathematics and Methods of Astrodynamics.* American Institute of Aeronautics and Astronautics, Inc., Reston, VA, revised edition, 1999.

[3] Steven C. Chapra. *Applied Numerical Methods with Matlab.* McGraw-Hill Companies, Inc., New York, NY, 1971.

[4] Hanspeter Schaub and John L. Junkins. *Analytical Mechanics of Space Systems.* American Institute of Aeronautics and Astronautics, Inc., Reston, VA, 2003.